

[6]

Pu IN COASTAL MARINE ENVIRONMENTS

PETER H. SANTSCHI, YUAN-HUI LI, JOY J. BELL, ROBERT M. TRIER and KATHY KAWTALUK

Lamont-Doherty Geological Observatory of Columbia University, Palisades, NY 10964 (U.S.A.)

Received April 21, 1980

Revised version received August 4, 1980

Analysis of water samples from the New York Bight area and Narragansett Bay reveals that a small fraction of the total Pu (probably Pu (III + IV) species) is continuously removed to the sediments at a rate similar to that of the particle-reactive isotope ^{228}Th . A more "soluble" Pu species appears to be released at times from the sediments to the water column in these nearshore regions. Sediments in shallow areas of the New York Bight south of Rhode Island and Narragansett Bay have high Pu inventories and relatively deep penetration of this element, although the net sediment accumulation rate is generally low ($<0.03 \text{ g/cm}^2 \text{ yr}$). The high Pu inventories can be explained if both sediment resuspension and sediment mixing are assumed to be the major controlling factors for the effective transfer of Pu from the water column to the sediments. By simultaneous modelling of the depth distribution of three tracers which operate on vastly different time scales: ^{234}Th (half-life 24 days), ^{210}Pb (half-life 22 years) and $^{239,240}\text{Pu}$ (introduced into the environment during the past 30 years), bioturbation rates ranging from 4 to $32 \text{ cm}^2/\text{yr}$ in the surface mixed layer (5–10 cm thick) and from 0.3 to $2.5 \text{ cm}^2/\text{yr}$ in the layer below (up to 40 cm thick) and net sediment accumulation rates of approximately zero to $0.14 \text{ g/cm}^2 \text{ yr}$ were calculated for these areas.

1. Introduction

The omnipresence of the plutonium isotopes ^{238}Pu , ^{239}Pu and ^{240}Pu (with respective half-lives of 88, 24×10^3 and 6540 years) in our environment is a result of atmospheric nuclear weapon tests. Accidental stratospheric injection of ^{238}Pu in 1964 resulting from the disintegration of a satellite nuclear auxiliary generator (SNAP-9A) increased the global ^{238}Pu fallout almost threefold [1]. Releases of plutonium isotopes from uranium fuel reprocessing plants are also responsible for the local contamination of coastal marine environments [2]. In light of the probable increased reliance on nuclear power, particularly breeder reactors, for energy production in the future, a deeper understanding of the biogeochemical behavior of transuranium nuclides in coastal environments is urgently needed. In this paper we present preliminary results of our study on the behavior of plutonium

isotopes in the water and sediments of the New York Bight and Narragansett Bay.

2. Materials and methods

Surface water samples from the New York Bight were collected in January 1976 (R/V "Conrad" 19-05) and in May 1977 (R/V "Cape Henlopen" CH-77-01). Narragansett Bay water was collected from the seawater line of the Aquarium building of the Graduate School of Oceanography, University of Rhode Island, Narragansett, R.I., from 1976 through 1978 (for a description of the sampling procedures see Santschi et al. [3]). In general, 200 gallons of surface seawater were acidified with 350 ml of concentrated HCl and spiked with appropriate amounts of ^{242}Pu (supplied by the EML Labs, New York) or ^{236}Pu tracers and 15–20 ml of FeCl_3 carrier. Appropriate amounts of ^{230}Th spike and BaCl_2 carrier were also added for subsequent Th and Ra analysis (Th and Ra results are presented in separate papers [3–5]). After 5–7 hours of equilibration 500 ml conc. NH_4OH

were added to precipitate amorphous $\text{Fe}(\text{OH})_3$, which coprecipitated Pu and Th isotopes. The precipitates were collected after 5–7 hours of settling, and chemically separated and analyzed for Pu according to Wong [6] and Simpson et al. [7], and for Th/Ra according to Broecker et al. [8].

Sediment samples were taken in August 1978 (R/V "Cape Henlopen"), either with a Soutar box corer (SBC-samples) or with a Hessler box corer (HBC-samples). Subcores were taken and sectioned immediately after collection; they were weighed, dried (at 80°C) and aliquots were taken soon after returning to the laboratory. In Narragansett Bay, cores were taken by divers in 1976 and 1977, 1 km north of Conanicut Island.

In general, 20–50 g of dry sediment were used for Pu, Th and U analysis, and 5 g for ^{210}Pb and ^{226}Ra analysis. The procedures used for $^{239,240}\text{Pu}$ analysis are similar to those of Wong [6] and Simpson et al. [7]. The ^{234}Th analyses were slightly modified from procedures described by Aller and Cochran [9], and the analysis of alpha-emitting Th and U isotopes were carried out according to Ku [10]. The ^{210}Pb analysis was similar to [11,12] and ^{226}Ra was analyzed according to Mathieu [13].

Sample preparation was as follows: 20 g of dried and pulverized sediment were leached with 100 ml hot conc. HNO_3 , 5 ml H_2O_2 (30%) and 10 g NaNO_2 for 2–3 hours for the analysis of Pu, Th and U isotopes following addition of a few dpm of ^{242}Pu as a yield tracer. The supernate was subsequently split into 75% and 25% aliquots; the 25% aliquots were left unspiked, the 75% aliquots were spiked with about 50 dpm of $^{232}\text{U}/^{228}\text{Th}$. U, Th and Pu were separated by anion exchange in 8N HNO_3 : U passed through the column in the 8N HNO_3 rinse solution, Th and Pu isotopes were adsorbed on the resin. Th was subsequently eluted with conc. HCl, and Pu with conc. HCl and NH_4I . The Pu fractions of the 75% and 25% aliquots were combined and analyzed together. Subsequent purification procedures which involve further separations on cation and anion exchange resins are described in the references given above. Th and U isotopes were evaporated on stainless steel discs as a TTA benzene extract, and Pu isotopes by electrodeposition. Discs were beta-counted in a gas flow counter for ^{234}Th (using a $15\text{ mg}/\text{cm}^2$ absorber) and alpha-counted in a surface barrier (silicon)

detector, coupled with a 200-channel multichannel analyzer for Th, U and Pu isotopes. Absolute activities of the isotopes under study were obtained by comparing their peaks with those of the yield tracers (^{232}U , ^{228}Th , ^{242}Pu or ^{236}Pu) after correcting for appropriate backgrounds, blanks, natural contributions (^{228}Th only) and radioactive decay. No significant blank corrections were necessary for Pu and U analysis. Alpha and beta detectors were calibrated using known amounts of ^{238}U (from NBS), $^{232}\text{Th}/^{228}\text{Th}$ (from Amersham/Searle) or ^{210}Pb (from EML Labs in New York), plated on discs. One of the authors (R.T.) has participated in a laboratory inter-comparison exercise [14]. Our analyses of river and marine sediments for $^{239,240}\text{Pu}$ and ^{238}Pu fell within the errors of the median value of all participating laboratories.

Samples for ^{210}Pb and ^{226}Ra analysis were leached with hot 6N HCl, and spiked with ^{208}Po yield tracers. The solution was subsequently diluted to 1.5N HCl, and plated onto a silver disc after adding ascorbic acid. The activity of ^{210}Pb was obtained by comparing the ^{210}Po and ^{208}Po peaks in the alpha spectrum, corrected for appropriate backgrounds, blanks and radioactive decay. The assumption of secular equilibrium between ^{210}Pb and ^{210}Po in the sediments was verified by analyzing a few samples separately for ^{210}Po and ^{210}Pb . The plating solution was later measured for ^{226}Ra by the ^{222}Rn method [13].

Even though thermodynamic considerations [15] favor the IV and VI oxidation states of Pu in natural waters, there is still some uncertainty over the predominant oxidation state for the III/IV or V/VI couples of Pu (see, for example, Wahlgren et al. [16] and Bondietti and Trabalka [17]). The analytical methods for separating the different oxidation states of Pu [16,18] do not distinguish between III and IV, nor between V and VI oxidation states. We therefore adopted the (III + IV), (V + VI) notation in the subsequent discussion of Pu oxidation states.

3. Results and discussion

3.1. $^{239,240}\text{Pu}$ in seawater

The $^{239,240}\text{Pu}$ concentrations of unfiltered surface waters from two New York Bight cruises are sum-

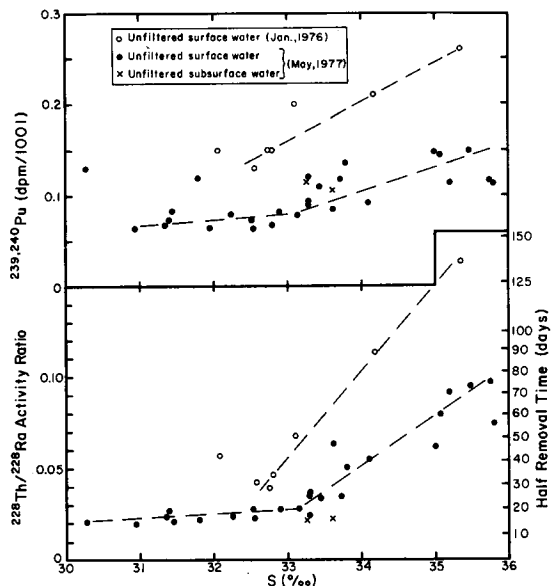


Fig. 1. Concentrations of $^{239,240}\text{Pu}$ and $^{228}\text{Th}/^{228}\text{Ra}$ activity ratios in water samples from the New York Bight versus salinity.

marized in Table 1. These data and the $^{228}\text{Th}/^{228}\text{Ra}$ activity ratios of these samples are plotted against salinity in Fig. 1. The daughter-parent ratio of $^{228}\text{Th}/^{228}\text{Ra}$ is a measure of the Th removal rate from the water column [8,19]. This is because Ra is relatively soluble in seawater, whereas Th is very "particle-reactive" and is removed rapidly from the water column of the New York Bight and Narragansett Bay [3-5,19,20]. Both the $^{239,240}\text{Pu}$ concentration and the $^{228}\text{Th}/^{228}\text{Ra}$ activity ratios decrease from the slope water (high-salinity region) toward the shore (lower salinity) (Fig. 1), while $^{239,240}\text{Pu}$ and $^{228}\text{Th}/^{228}\text{Ra}$ are somehow linearly correlated (Fig. 2). Thus it is likely that the mechanism which removes Th from the water column (thereby controlling the $^{228}\text{Th}/^{228}\text{Ra}$ activity ratios), also removes a fraction of the Pu. This mechanism requires a sorption step onto suspended particles and the settling of these particles [3-5,19]. As a major transport mechanism for removal of ^{228}Th from the waters of the New York Bight, Li et al. [5] suggest adsorption on non-living particles (detritus), originating from resuspension of surface sediments. The same removal mechanism could also apply to $^{239,240}\text{Pu}$ removal. The conclusion of Li et al. [5] is based mainly on significant

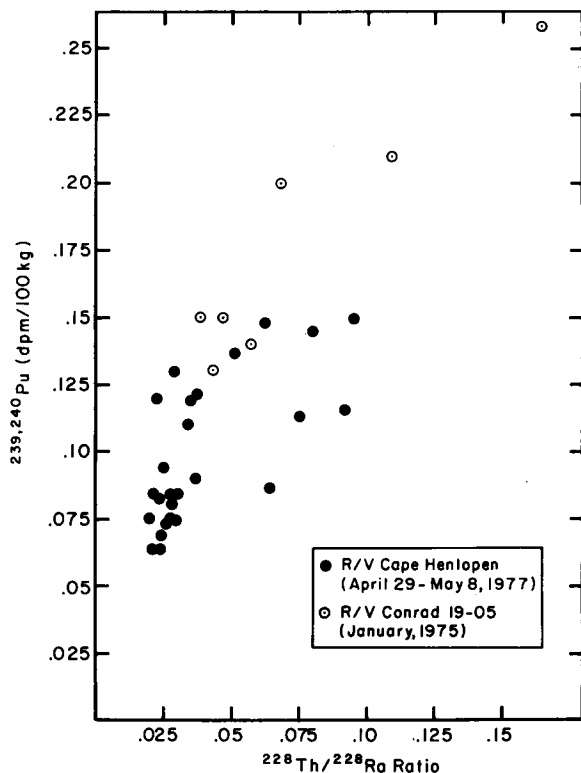


Fig. 2. Correlation of $^{239,240}\text{Pu}$ concentrations with $^{228}\text{Th}/^{228}\text{Ra}$ activity ratios in water samples of the New York Bight.

positive correlation of removal rates of ^{228}Th with the concentrations of ^{232}Th (which is an indicator of inorganic detritus). Furthermore, no correlation of ^{228}Th removal rates with chlorophyll-a concentrations in the water samples, during times when zooplankton grazing was insignificant, has been found. The importance of zooplankton grazing as a mechanism for Pu removal can be estimated the following way. Using the Pu concentrations in fecal pellets of 0.3 dpm/g [21], an average feeding rate of $0.3 \times$ body weight per day, a food utilization of 50% of carbon intake (both from Lowman et al. [22] and references therein) and an average zooplankton standing crop of 1 g/m² in the shelf area of the New York Bight (calculated from Walsh et al. [23]), we arrive at a removal rate of 1.6×10^{-3} dpm/cm² yr. This figure is considerably smaller than the total Pu removal rate calculated from ^{228}Th removal (see below). It appears, therefore, that zooplankton grazing is not

TABLE 1

Concentration of $^{239,240}\text{Pu}$ in the New York Bight (unfiltered surface and subsurface water)

Ship station	Latitude N	Longitude W	Salinity (‰)	Temperature (°C)	$^{239,240}\text{Pu}$ (dpm/100 kg)
<i>R/V "Cape Henlopen", April 29 to May 8, 1977</i>					
1	39° 31'	74° 09'	30.27	8.98	0.130 ± 0.011
2	39° 27'	73° 56'	31.39	9.55	0.074 ± 0.006
4	39° 15'	73° 27'	33.63	9.79	0.086 ± 0.008
4 (25 m)	39° 15'	73° 27'	34.09	5.90	0.093 ± 0.012
7	39° 04'	72° 50'	33.80	8.97	0.137 ± 0.015
8	39° 02'	72° 33'	35.01	12.70	0.148 ± 0.025
9	38° 31'	71° 42'	35.80	13.60	0.113 ± 0.011
10	38° 47'	72° 10'	35.47	13.58	0.149 ± 0.013
14	39° 18'	71° 49'	35.07	13.33	0.145 ± 0.012
14 (28 m)	39° 18'	71° 49'	35.76	13.48	0.117 ± 0.016
16	39° 33'	71° 26'	~35.20	~13.30	0.115 ± 0.013
17	39° 40'	72° 29'	33.30	9.84	0.090 ± 0.012
18	39° 39'	72° 43'	33.15	10.10	0.080 ± 0.010
19	39° 53'	72° 40'	32.79	9.03	0.068 ± 0.007
20	39° 46'	72° 57'	32.53	8.95	0.075 ± 0.009
22	39° 55'	73° 13'	32.54	9.09	0.064 ± 0.007
27	40° 09'	73° 11'	32.90	9.18	0.084 ± 0.011
29	40° 23'	73° 02'	31.45	9.40	0.085 ± 0.008
30	40° 30'	72° 37'	31.81	8.96	0.120 ± 0.010
31	40° 47'	72° 29'	31.34	9.36	0.068 ± 0.008
32	40° 41'	72° 20'	30.94	9.09	0.065 ± 0.003
33	40° 37'	72° 13'	31.96	9.75	0.065 ± 0.004
34	40° 27'	72° 05'	32.26	9.77	0.082 ± 0.008
34 (21 m)	40° 27'	72° 05'	33.27	4.05	0.116 ± 0.014
35	40° 19'	71° 58'	33.30	9.12	0.075 ± 0.008
35 (40 m)	40° 19'	71° 58'	33.61	4.52	0.088 ± 0.012
36	40° 12'	71° 53'	33.30	9.30	0.094 ± 0.005
36 (45 m)	40° 12'	71° 53'	33.62	4.51	0.107 ± 0.007
37	40° 02'	71° 50'	33.45	9.97	0.110 ± 0.013
42	40° 00'	71° 44'	33.31	9.62	0.121 ± 0.009
43	39° 51'	71° 32'	33.73	10.90	0.119 ± 0.014
47 (50 m)	39° 50'	71° 30'	35.50	12.50	0.079 ± 0.006
<i>R/V "Conrad", January 1976</i>					
100	40° 27'	72° 06'	32.570	8.26	0.13 ± 0.02
104	39° 58'	71° 43'	33.111	9.20	0.20 ± 0.02
125	38° 46'	71° 57'	35.347	13.43	0.26 ± 0.03
136	40° 12'	73° 43'	32.071	6.08	0.14 ± 0.01
141	39° 44'	73° 14'	32.814	7.17	0.15 ± 0.02
148	39° 34'	73° 03'	32.807	7.21	0.15 ± 0.02
166	39° 22'	72° 34'	33.874	9.90	0.21 ± 0.03

the dominant removal pathway. Our removal model for Pu as described above is different from previously published models for removal of Pu from the ocean [24–26]. They are based on the vertical transport of

Pu attached to different populations of particles, settling at various velocities.

The few samples closest to the shore, with relatively high Pu concentrations, are exceptions to this

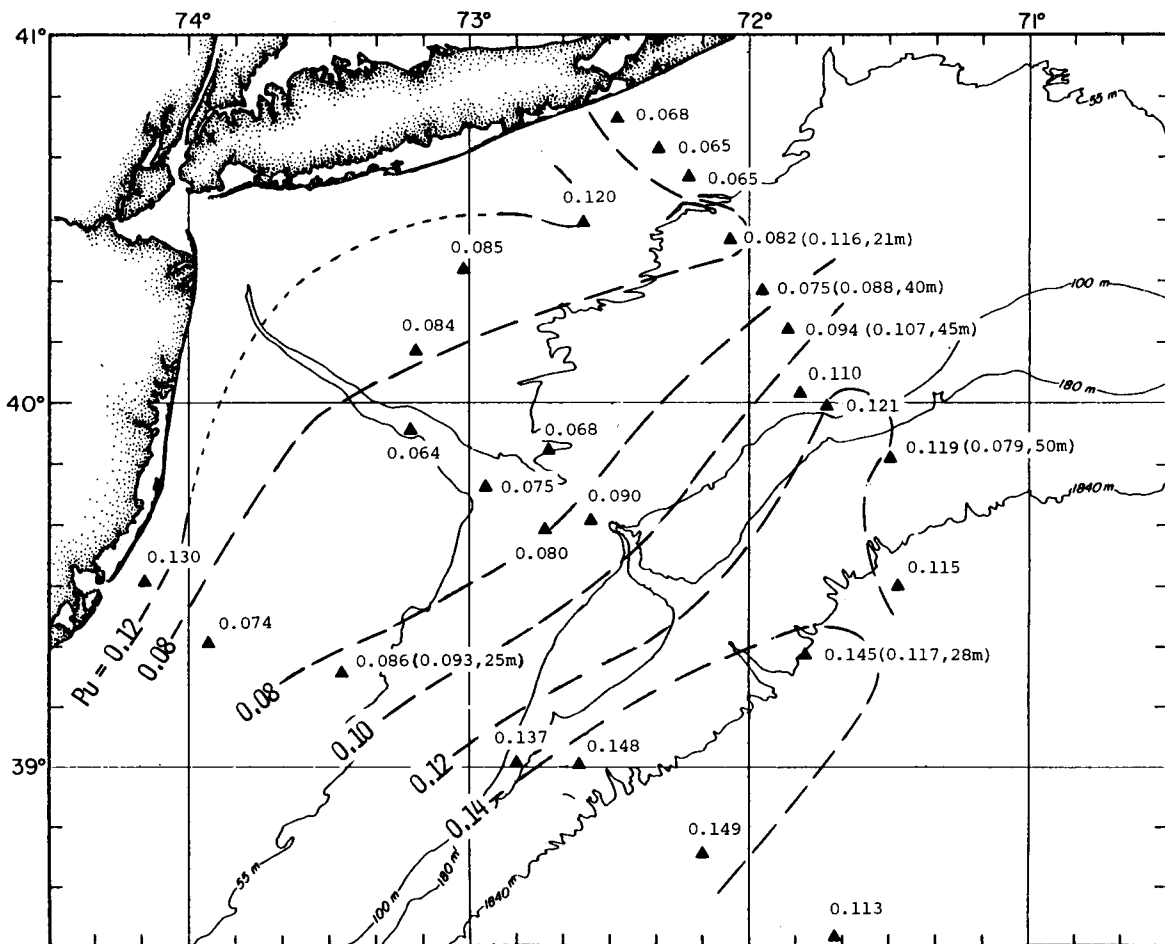


Fig. 3. Concentrations of $^{239,240}\text{Pu}$ in surface water samples of the New York Bight (R/V "Cape Henlopen", April 29 to May 8, 1977).

$^{239,240}\text{Pu}$ - $^{228}\text{Th}/^{228}\text{Ra}$ correlation (Fig. 1). One would expect the high Pu concentration near shore (Fig. 3) to be related to the high suspended particle concentration there. However, a suspended particle sample ($>0.45\ \mu\text{m}$) collected in the same nearshore area contained a specific concentration of about 0.04 dpm $^{239,240}\text{Pu}/\text{g}$ and the suspended particle concentration there was about 0.05 g/100 l. The concentration of Pu on suspended particles is therefore only about 0.002 dpm/100 l (a few percent of the total concentration) which is not large enough to explain the higher Pu concentration near shore. The influence of Hudson river $^{239,240}\text{Pu}$ inputs is negligible, since concentrations of dissolved $^{239,240}\text{Pu}$ in the Hudson

River water are lower than those found in the New York Bight area [7]. This fact suggests that an unreactive Pu species, possibly an anionic Pu (V + VI) species [15,18], may be injected into the water column from the nearshore sediments. Nelson and Lovett [18] have shown that about 85% of $^{239,240}\text{Pu}$ in the water of the Irish Sea is present as a relatively unreactive, anionic Pu (V + VI) species, and only approximately 15–20% as the "particle-reactive", highly hydrolysable Pu (III + IV). They report furthermore that the distribution coefficient between particles and water is up to 1000 times greater for Pu (III + IV) than for Pu(V + VI).

In order to study further the cycling of Pu in

TABLE 2

Results from the $^{239,240}\text{Pu}$ analysis in the water of Narragansett Bay (Aquarium seawater line at the Graduate School of Oceanography, University of Rhode Island, Narragansett, R.I.)

Date	Particulate matter concentration (mg/l)	Temperature ($^{\circ}\text{C}$)	Salinity (‰)	Sample characteristics	$^{239,240}\text{Pu}$ (dpm/100 kg)
6/1/76	6.5 ± 0.5	14.7	30.9	unfiltered	0.18 ± 0.02
7/15/76	6.6 ± 0.5	21.5	31.1	unfiltered	0.17 ± 0.02
9/28/76	5.0 ± 1	17.2	30.3	unfiltered filtered ($\leq 5 \mu\text{m}$)	0.12 ± 0.01 0.085 ± 0.01
12/1/76	5.2 ± 0.5	4.5	32.2	unfiltered filtered ($\leq 0.45 \mu\text{m}$)	0.19 ± 0.02 0.14 ± 0.01
4/19/77	4.1 ± 0.5	8.5	30.0	unfiltered filtered ($\leq 0.45 \mu\text{m}$)	0.065 ± 0.01 0.08 ± 0.01
7/25/77	9.5 ± 1	21.4	30.0	unfiltered filtered ($\leq 0.45 \mu\text{m}$)	0.265 ± 0.015 0.25 ± 0.05
11/15/77	10.5 ± 1	11.0	30.0	unfiltered filtered ($\leq 0.45 \mu\text{m}$)	0.19 ± 0.05 0.14 ± 0.05
7/25/78	6.8 ± 0.5	22.0	30.3	unfiltered filtered ($\leq 0.45 \mu\text{m}$)	0.136 ± 0.008 0.139 ± 0.015

coastal waters, we performed a series of experiments with Narragansett Bay waters. We analyzed $^{239,240}\text{Pu}$ along with other natural radionuclides [3] in both unfiltered and filtered ($<0.45 \mu\text{m}$) water samples. The $^{239,240}\text{Pu}$ results are given in Table 2 and are plotted against the suspended particle concentration in Fig. 4. Though the temporal variations in water column inventories are dramatic, they are insignificant (less than 1%) compared to the sediment inventory (see later section). The particulate Pu activity ($>0.45 \mu\text{m}$) is calculated by subtracting the filtrate activity from the total. The dashed lines in Fig. 4 represent the predicted concentrations of particulate Pu and ^{234}Th (dpm/100 kg of water) if the particulate matter in the water column is composed entirely of resuspended surface sediments. It is evident from Fig. 4 that the concentrations of total, and filterable ($<0.45 \mu\text{m}$) $^{239,240}\text{Pu}$ in the water of Narragansett Bay increase with the suspended particle concentration. The increase in the total or filterable fractions again cannot be explained by the direct contribution of suspended particles ($>0.45 \mu\text{m}$) alone. It is important to note that in Narragansett Bay, while the concentrations of "soluble" $^{239,240}\text{Pu}$ correlate positively with

the concentrations of suspended particles as stated above, the opposite was found for "particle-reactive" ^{234}Th (see Santschi et al. [3] and Fig. 4). High suspended matter and Pu concentrations were observed only during summer and fall seasons, when rates of resuspension of surface sediments were high as well [3,20]. Pu appears, therefore, to be released into the

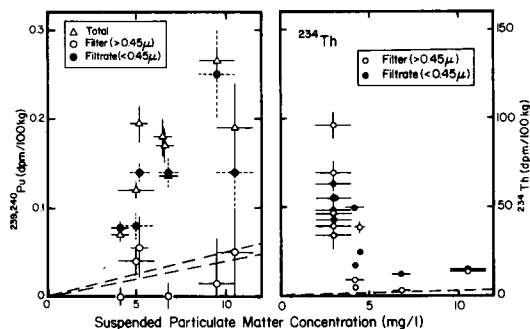


Fig. 4. Concentrations of $^{239,240}\text{Pu}$ and ^{234}Th [3] in water samples of Narragansett Bay (on filter ($>0.45 \mu\text{m}$) and in filtrate ($<0.45 \mu\text{m}$)) versus the particulate matter concentrations. Dashed lines indicate expected concentrations if the particulate matter has the same activity as the surface sediments.

water column, perhaps in the form of soluble (V + VI) or as an apparently soluble Pu (III + IV) colloid. So far, there are few convincing examples of back-diffusion of Pu from marine sediments (e.g. [26]).

Assuming that the Pu speciation in the New York Bight is similar to the Irish Sea [18], we attempted to estimate the removal flux to the sediments. If the average half removal times (t_c) of the particle-reactive $^{239,240}\text{Pu}$ (III + IV) in the water column (15–20% of the total) is similar to ^{228}Th , i.e., about 22 days [4,5,19], and the conversion of Pu (V, VI) to Pu (III, IV) is rapid, an apparent flux of $^{239,240}\text{Pu}$ from the shelf water column to the bottom sediments can be estimated to be about $(7\text{--}14) \times 10^{-3}$ dpm/cm² yr ($= (\ln 2/t_c) \cdot [\text{Pu}]_{\text{shelf}} \cdot h \cdot 0.05$), where the average $^{239,240}\text{Pu}$ concentration of shelf water, $[\text{Pu}]_{\text{shelf}}$, is about 0.1 ± 0.05 dpm/100 kg, h = average depth of the shelf water = 50 m, $t_c = 22 \pm 5$ days. In steady state, this flux should be balanced by inputs from atmospheric deposition, rivers and open ocean waters. The mean annual atmospheric deposition of ^{90}Sr from 1972 through 1976 averaged 0.9% of the cumulative deposition [27]. Assuming the same ratio for $^{239,240}\text{Pu}$, atmospheric deposition of $^{239,240}\text{Pu}$ during this time amounts to $(4 \pm 1) \times 10^{-3}$ dpm/cm² yr. According to Simpson et al. [7], the average concentrations of “dissolved” ($<0.45 \mu\text{m}$) and particulate ($>0.45 \mu\text{m}$) $^{239,240}\text{Pu}$ concentrations in the Hudson River are about 0.066 dpm/100 kg water and 0.044 dpm/g sediment, respectively. Since the streamflow per unit area of shelf (<100 m isobath) on the Middle Atlantic Bight is about 160 cm/yr [28], and the average sedimentation rate for this area is probably not greater than 0.01 g/cm² yr (the sedimentation rate will be discussed in a later section), the “dissolved” $^{239,240}\text{Pu}$ input of rivers to the Middle Atlantic Bight is about 0.1×10^{-3} dpm/cm² yr, and the particulate input of $^{239,240}\text{Pu}$ not more than 0.4×10^{-3} dpm/cm² yr. The $^{239,240}\text{Pu}$ flux from the slope to the shelf water by water exchange in the Middle Atlantic Bight, F_x is about $(2.5 \pm 1.5) \times 10^{-3}$ dpm/cm² yr, as calculated by the following equation:

$$F_x = (Q_x/A) \cdot ([\text{Pu}]_{\text{slope}} - [\text{Pu}]_{\text{shelf}})$$

where Q_x = water exchange rate between the slope and shelf = 2500 ± 800 km³/yr [19], A = area of the Middle Atlantic Bight within 100-m isobath = 98×10^9 m² [28], $[\text{Pu}]_{\text{slope}} - [\text{Pu}]_{\text{shelf}}$ = $^{239,240}\text{Pu}$ con-

centration difference between slope and shelf waters = 0.1 ± 0.03 dpm/100 kg (see Fig. 1). The total inputs to the shelf waters are then approximately $(7 \pm 2) \times 10^{-3}$ dpm/cm² yr. Therefore, it seems that the $^{239,240}\text{Pu}$ flux to the shelf sediments is approximately balanced by inputs from atmosphere, rivers and open ocean. Since the standing crop of $^{239,240}\text{Pu}$ in the average shelf water column (50 m) is about 5×10^{-3} dpm/cm², the residence time of $^{239,240}\text{Pu}$ in the shelf water column with respect to removal to the sediments is about 1–3 years. Wahlgren et al. [29] report a $^{239,240}\text{Pu}$ residence time of 2.5 years in the water of Lake Michigan, which has a similar mean depth (84 m) and fractionation of dissolved Pu (III + IV)/Pu (V + VI) (~ 0.2).

The concentrations of $^{239,240}\text{Pu}$ in the nearshore waters are maintained at levels similar to those found for surface waters of the Atlantic Ocean, measured between 1963 and 1970, i.e., 0.04–0.31 dpm/100 kg [6,30], even though a significant fraction of the fall-

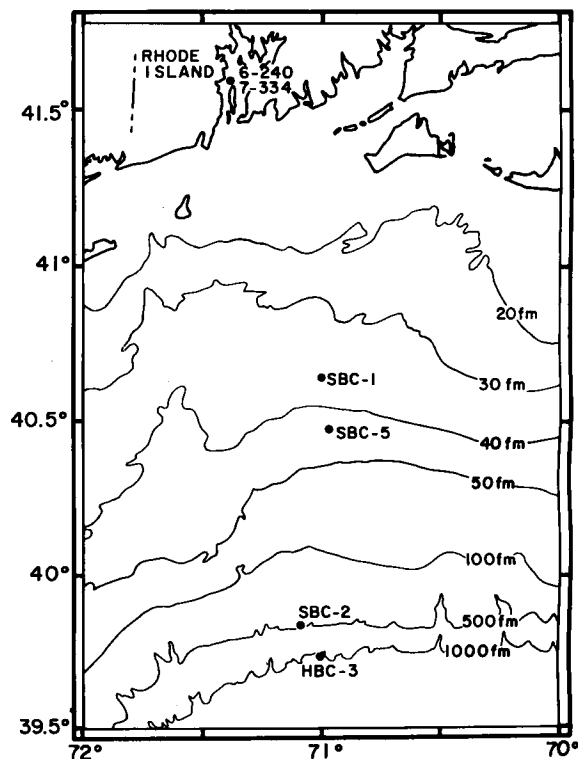


Fig. 5. Location of the sediment cores from the New York Bight and Narragansett Bay.

TABLE 3

Results from radionuclide analysis of sediments (errors are expressed as 1 standard deviation)

Depth interval (cm)	Porosity ϕ	$^{234}\text{Th}_{\text{xs}}$ (dpm/g)	^{232}Th (dpm/g)	^{230}Th (dpm/g)	^{228}Th (dpm/g)	^{238}U (dpm/g)	$^{234}\text{U}/^{238}\text{U}$	$^{226}\text{Ra}^{**}$ (dpm/g)	$^{210}\text{Pb}_{\text{xs}}$ (dpm/g)	$^{239,240}\text{Pu}$ (dpm/kg)	^{238}Pu (dpm/kg)
<i>Core SBC-1</i> , location 40°38'N, 71°00'W (CH-B.T.-44, "mud-hole"), 16 August 1978, water depth = 69 m											
0 - 0.6	0.76	10.75 ± 0.76	2.13 ± 0.09	1.43 ± 0.07	1.91 ± 0.14	1.02 ± 0.07	1.07 ± 0.09	-	5.69 ± 0.27	81.6 ± 7.1	-
0.6 - 1.3	0.76	4.24 ± 0.34	1.82 ± 0.09	1.27 ± 0.06	1.69 ± 0.10	-	-	-	5.28 ± 0.28	74.4 ± 4.4	3.31 ± 0.71
1.3 - 2.5	0.71	0.91 ± 0.26	1.94 ± 0.11	1.33 ± 0.08	1.66 ± 0.11	1.02 ± 0.07	1.08 ± 0.07	-	5.36 ± 0.31	82.4 ± 3.6	4.64 ± 0.67
2.5 - 3.8	0.70	-	1.82 ± 0.10	1.32 ± 0.08	1.58 ± 0.10	-	-	0.59 ± 0.03	5.32 ± 0.29	74.2 ± 3.3	2.62 ± 0.42
3.8 - 5.1	0.69	-0.54 ± 0.21	-	-	-	0.99 ± 0.07	1.06 ± 0.07	-	5.57 ± 0.29	85.6 ± 5.3	3.58 ± 0.76
5.1 - 6.4	0.69	-	-	-	-	-	-	-	5.49 ± 0.22	94.9 ± 4.4	3.87 ± 0.56
6.4 - 7.0	0.69	-	-	-	-	-	-	-	5.49 ± 0.29	107.6 ± 4.7	4.11 ± 0.58
8.9 - 10.2	0.64	-	-	-	-	-	-	-	3.67 ± 0.19	67.6 ± 2.7	2.93 ± 0.31
10.2 - 11.4	0.60	-	-	-	-	-	-	-	-	50.6 ± 2.0	2.38 ± 0.27
11.4 - 12.7	0.56	-	-	-	-	-	-	-	1.54 ± 0.13	23.6 ± 1.3	0.91 ± 0.27
14.0 - 15.2	0.53	-	-	-	-	-	-	-	2.00 ± 0.15	16.2 ± 0.7	0.71 ± 0.13
16.5 - 17.7	0.58	-	-	-	-	-	-	-	1.27 ± 0.12	19.8 ± 1.1	0.56 ± 0.16
19.0 - 20.3	0.59	-	-	-	-	-	-	-	0.96 ± 0.12	13.7 ± 0.7	0.67 ± 0.20
22.9 - 24.1	0.58	-	1.75 ± 0.07	1.21 ± 0.06	1.79 ± 0.10	1.37 ± 0.05	1.11 ± 0.03	-	-	-	-
24.2 - 25.4	0.56	-	-	-	-	-	-	-	0.13 ± 0.11	1.8 ± 0.2	n.d.
26.7 - 27.9	0.55	-	1.64 ± 0.06	1.16 ± 0.05	1.56 ± 0.08	1.78 ± 0.05	1.05 ± 0.02	-	-	-	-
29.2 - 30.4	0.55	-	-	-	-	-	-	-	0.17 ± 0.11	1.9 ± 0.2	n.d.
31.7 - 33.0	0.52	-	1.46 ± 0.07	1.52 ± 0.06	1.39 ± 0.09	1.32 ± 0.07	1.02 ± 0.05	-	0.05 ± 0.09	0.26 ± 0.02	n.d.
<i>Core SBC-5</i> , location 40°28.1'N, 70°58.0'W (CH-B.T.-58, "mud-hole"), 18 August 1978, water depth = 87 m											
0 - 0.6	0.80	8.07 ± 0.48	1.58 ± 0.09	1.12 ± 0.07	1.46 ± 0.10	0.91 ± 0.04	1.07 ± 0.04	-	8.42 ± 0.40	80.7 ± 5.1	3.58 ± 0.89
0.6 - 1.3	0.78	2.61 ± 0.23	1.68 ± 0.09	1.13 ± 0.07	1.54 ± 0.11	0.95 ± 0.07	0.94 ± 0.10	-	8.26 ± 0.43	81.6 ± 6.4	6.58 ± 1.47
1.3 - 1.9	0.77	1.12 ± 0.15	1.71 ± 0.10	1.26 ± 0.08	1.66 ± 0.11	0.93 ± 0.05	0.98 ± 0.06	0.49 ± 0.02	8.19 ± 0.39	80.2 ± 6.7	5.78 ± 1.40
1.9 - 2.5	0.76	-0.65 ± 0.10	1.67 ± 0.10	1.07 ± 0.08	1.55 ± 0.11	1.07 ± 0.05	1.00 ± 0.05	0.77 ± 0.01	8.25 ± 0.43	80.0 ± 4.7	3.00 ± 0.73
2.5 - 3.8	0.75	-0.11 ± 0.22	1.68 ± 0.10	1.25 ± 0.08	1.47 ± 0.10	1.30 ± 0.04	1.03 ± 0.03	0.54 ± 0.02	6.86 ± 0.40	85.5 ± 5.6	5.58 ± 1.04
3.8 - 5.1	0.74	0.19 ± 0.29	1.80 ± 0.10	1.16 ± 0.07	1.50 ± 0.10	1.05 ± 0.05	1.12 ± 0.05	0.32 ± 0.01	6.93 ± 0.34	76.7 ± 6.4	2.27 ± 0.87
5.1 - 6.4	0.72	-	-	-	-	-	-	0.42 ± 0.02	6.42 ± 0.24	80.9 ± 2.7	3.24 ± 0.73
6.4 - 7.6	0.70	-	-	-	-	-	-	0.45 ± 0.02	5.72 ± 0.22	79.3 ± 2.2	2.98 ± 0.31
7.6 - 8.9	0.69	-	-	-	-	-	-	0.31 ± 0.02	5.02 ± 0.21	61.8 ± 2.0	3.07 ± 0.33
8.9 - 10.2	0.68	-	-	-	-	-	-	-	4.83 ± 0.20	53.6 ± 2.0	2.02 ± 0.40
10.2 - 11.4	0.68	-	-	-	-	-	-	-	4.60 ± 0.20	60.2 ± 2.7	2.13 ± 0.29
11.4 - 12.7	0.68	-	-	-	-	-	-	0.56 ± 0.03	4.83 ± 0.20	55.6 ± 2.4	1.62 ± 0.31
14.0 - 15.2	0.68	-	-	-	-	-	-	-	3.57 ± 0.17	9.7 ± 0.5	0.49 ± 0.15
16.5 - 17.8	0.68	-	-	-	-	-	-	-	2.21 ± 0.13	-	n.d.
19.0 - 20.3	0.68	-	-	-	-	-	-	-	1.89 ± 0.15	2.6 ± 0.3	n.d.
21.6 - 22.9	0.63	-	-	-	-	-	-	-	1.71 ± 0.13	13.3 ± 0.7	n.d.
24.1 - 25.4	0.60	-	-	-	-	-	-	-	1.01 ± 0.12	12.7 ± 0.5	n.d.

TABLE 3 (continued)

Depth interval (cm)	Porosity ϕ	$^{234}\text{Th}_{\text{xs}}$ (dpm/g)	^{232}Th (dpm/g)	^{230}Th (dpm/g)	^{228}Th (dpm/g)	^{238}U (dpm/g)	$^{234}\text{U}/^{238}\text{U}$	$^{226}\text{Ra}^{**}$ (dpm/g)	$^{210}\text{Pb}_{\text{xs}}$ (dpm/g)	$^{239,240}\text{Pu}$ (dpm/kg)	^{238}Pu (dpm/kg)
<i>Core SBC-2</i> *, location 39° 50.0'N, 71° 05.2'W (CH-B.T.-48, slope), 17 August 1978, water depth = 850 m											
0 - 1.3	0.70	8.03 ± 0.46	1.52 ± 0.09	1.65 ± 0.09	1.75 ± 0.13	0.67 ± 0.05	1.03 ± 0.09	-	18.62 ± 0.93	38.0 ± 3.3	1.76 ± 0.60
1.3 - 1.9	0.70	0.74 ± 0.24	1.59 ± 0.10	1.54 ± 0.10	1.60 ± 0.12	0.71 ± 0.05	1.00 ± 0.10	0.35 ± 0.01	12.41 ± 0.58	30.0 ± 2.7	1.82 ± 0.58
1.9 - 2.5	0.66	-0.13 ± 0.18	1.55 ± 0.07	1.50 ± 0.07	1.29 ± 0.09	0.74 ± 0.04	0.99 ± 0.05	-	8.14 ± 0.33	14.4 ± 2.0	n.d.
2.5 - 3.4	0.64	-0.13 ± 0.13	1.24 ± 0.06	1.38 ± 0.07	0.98 ± 0.07	0.68 ± 0.04	1.06 ± 0.05	0.38 ± 0.02	6.40 ± 0.29	13.3 ± 1.1	n.d.
3.4 - 4.2	0.62	-	1.27 ± 0.06	1.49 ± 0.06	1.04 ± 0.06	0.76 ± 0.03	1.01 ± 0.04	0.51 ± 0.02	4.91 ± 0.23	7.4 ± 0.3	0.76 ± 0.24
4.2 - 5.1	0.62	0.24 ± 0.39	1.58 ± 0.11	1.44 ± 0.10	1.26 ± 0.12	1.07 ± 0.06	1.08 ± 0.05	0.53 ± 0.02	4.28 ± 0.24	3.8 ± 0.4	0.93 ± 0.24
5.1 - 6.4	0.61	-	-	-	-	-	-	3.09 ± 0.14	-	-	-
6.4 - 7.6	0.61	-	-	-	-	-	-	0.72 ± 0.02	3.01 ± 0.15	-	-
7.6 - 8.9	-	-	-	-	-	-	-	-	-	3.5 ± 0.2	n.d.
8.9 - 10.2	0.61	-	-	-	-	-	-	-	2.24 ± 0.12	2.1 ± 0.2	n.d.
11.4 - 12.7	0.60	-	-	-	-	-	-	0.47 ± 0.01	1.80 ± 0.10	-	-
14.0 - 15.2	0.63	-	-	-	-	-	-	-	1.21 ± 0.09	0.62 ± 0.09	n.d.
16.5 - 17.8	0.62	-	-	-	-	-	-	0.49 ± 0.01	0.97 ± 0.09	-	-
21.6 - 22.9	0.63	-	1.75 ± 0.09	1.71 ± 0.09	1.77 ± 0.10	-	-	-	0.89 ± 0.07	-	n.d.
26.7 - 27.9	0.62	-	1.94 ± 0.08	1.71 ± 0.07	2.03 ± 0.10	0.86 ± 0.07	1.04 ± 0.10	-	1.38 ± 0.09	-	-
31.7 - 33.0	0.63	-	-	-	-	-	-	-	0.85 ± 0.07	-	-
34.3 - 35.6	-	-	1.90 ± 0.08	1.74 ± 0.07	2.00 ± 0.11	1.05 ± 0.31	1.19 ± 0.51	-	-	n.d.	n.d.
<i>Core HBC-3</i> *, location 39° 44.2'N, 71° 02.0'W (CH-B.T.-49, slope), 17 August 1978, water depth = 1800 m											
0 - 0.2	~1	1.43 ± 0.26	1.34 ± 0.06	2.47 ± 0.11	1.33 ± 0.09	0.74 ± 0.06	1.10 ± 0.09	-	25.52 ± 1.39	31.3 ± 4.4	2.4 ± 0.7
0.2 - 1.1	0.8	0.22 ± 0.12	1.48 ± 0.06	2.42 ± 0.10	1.44 ± 0.08	0.85 ± 0.10	1.34 ± 0.14	-	17.78 ± 0.66	27.3 ± 1.6	2.0 ± 0.35
1.1 - 2.1	0.79	0.09 ± 0.29	1.46 ± 0.28	2.64 ± 0.11	1.43 ± 0.10	0.85 ± 0.07	1.14 ± 0.10	-	17.47 ± 0.89	25.8 ± 2.2	4.1 ± 0.6
2.1 - 3.0	0.78	-	1.59 ± 0.11	2.66 ± 0.17	1.38 ± 0.12	1.22 ± 0.05	1.09 ± 0.03	1.16 ± 0.06	9.22 ± 0.61	11.4 ± 1.6	n.d.
3.0 - 4.0	0.78	0.06 ± 0.30	1.69 ± 0.09	3.00 ± 0.16	1.54 ± 0.10	1.20 ± 0.06	1.06 ± 0.04	0.93 ± 0.05	7.74 ± 0.46	10.4 ± 1.7	n.d.
4.0 - 4.9	0.77	-	1.54 ± 0.11	2.49 ± 0.18	1.46 ± 0.25	-	-	-	6.36 ± 0.25	6.5 ± 1.2	n.d.
4.9 - 5.8	0.77	-0.10 ± 0.35	1.50 ± 0.10	2.45 ± 0.15	1.29 ± 0.10	1.09 ± 0.04	1.11 ± 0.03	-	7.33 ± 0.30	7.7 ± 1.0	n.d.
5.8 - 6.8	0.74	-	-	-	-	-	-	0.99 ± 0.05	12.50 ± 0.47	15.8 ± 2.0	n.d.
6.8 - 7.8	0.74	-	-	-	-	-	-	-	-	-	-
7.8 - 8.8	0.76	-	-	-	-	-	-	-	17.15 ± 0.10	12.4 ± 2.0	n.d.
8.8 - 9.8	0.76	-	-	-	-	-	-	-	-	3.55 ± 0.45	n.d.
9.8 - 10.8	0.70	-	-	-	-	-	-	-	4.99 ± 0.22	-	-
11.8 - 12.8	0.70	-	-	-	-	-	-	-	1.66 ± 0.13	-	-
13.8 - 14.8	0.72	-	-	-	-	-	-	-	1.30 ± 0.11	n.d.	-

TABLE 3 (continued)

Depth interval (cm)	Porosity ϕ	^{232}Th (dpm/g)	^{230}Th (dpm/g)	^{228}Th (dpm/g)	^{238}U (dpm/g)	$^{234}\text{U}/^{238}\text{U}$	^{226}Ra (dpm/g)	$^{210}\text{Pb}_{\text{xs}}$ (dpm/g)	$^{239,240}\text{Pu}$ (dpm/kg)	
<i>Core 6-240-00-900, location 41° 35'N, 71° 22.3'W (ca. 1 km north of Conanicut Island, Narragansett Bay), 27 August 1976, water depth = 10 m</i>										
0-5	0.61	1.90 ± 0.11	1.35 ± 0.10	1.34 ± 0.08	-	-	0.76 ± 0.02	2.19 ± 0.27	49 ± 3	
5-10	0.58	2.00 ± 0.08	1.22 ± 0.06	1.77 ± 0.07	-	-	0.79 ± 0.03	1.45 ± 0.17	39 ± 2	
10-15	0.59	2.15 ± 0.08	1.34 ± 0.05	1.88 ± 0.07	-	-	0.85 ± 0.04	0.56 ± 0.12	28 ± 2	
15-20	0.62	1.88 ± 0.10	1.12 ± 0.07	1.77 ± 0.10	-	-	0.92 ± 0.04	0.21 ± 0.10	15 ± 1	
20-25	0.56	1.99 ± 0.04	1.21 ± 0.22	1.87 ± 0.04	-	-	0.79 ± 0.06	0.35 ± 0.11	13 ± 1	
25-30	0.54	-	-	-	-	-	0.85 ± 0.07	0.10 ± 0.07	-	
30-35	0.52	-	-	-	-	-	0.79 ± 0.02	0.09 ± 0.09	-	
35-40	-	-	-	-	-	-	1.20 ± 0.08	0.12 ± 0.12	n.d.	
Depth interval (cm)	Porosity ϕ	$^{234}\text{Th}_{\text{xs}}$ (dpm/g)	^{232}Th (dpm/g)	^{230}Th (dpm/g)	^{228}Th (dpm/g)	^{238}U (dpm/g)	$^{234}\text{U}/^{238}\text{U}$	^{226}Ra ** (dpm/g)	$^{210}\text{Pb}_{\text{xs}}$ (dpm/g)	$^{239,240}\text{Pu}$ (dpm/kg)
<i>Core 7-334-00-900, location 41° 35'N, 71° 22.3'W (ca. 1 km north of Conanicut Island, Narragansett Bay), 30 November 1977, water depth = 10 m</i>										
0-1	0.88	7.11 ± 0.82	2.13 ± 0.09	1.70 ± 0.07	1.69 ± 0.09	1.29 ± 0.05	0.93 ± 0.04	0.80 ± 0.04	1.84 ± 0.13	42.7 ± 2.0
1-2	0.75	0.84 ± 0.51	1.87 ± 0.09	1.31 ± 0.05	1.57 ± 0.09	1.20 ± 0.04	1.09 ± 0.03	0.80 ± 0.04	2.00 ± 0.17	42.7 ± 2.0
2-3	0.74	-	1.99 ± 0.09	1.39 ± 0.05	1.75 ± 0.09	1.27 ± 0.05	1.03 ± 0.03	0.80 ± 0.04	1.88 ± 0.12	42.7 ± 2.0
3-4	0.74	0.96 ± 0.51	1.86 ± 0.09	1.18 ± 0.06	1.66 ± 0.09	1.34 ± 0.05	1.05 ± 0.03	0.80 ± 0.04	1.75 ± 0.12	42.7 ± 2.0
4-5	0.73	-	2.10 ± 0.09	1.33 ± 0.06	1.63 ± 0.04	1.39 ± 0.04	1.05 ± 0.02	0.80 ± 0.04	1.87 ± 0.10	42.7 ± 2.0
5-6	0.71	0.06 ± 0.41	1.94 ± 0.08	1.25 ± 0.05	1.58 ± 0.07	1.38 ± 0.06	1.07 ± 0.04	0.80 ± 0.04	1.61 ± 0.09	42.7 ± 2.0
6-10	0.67	-	1.95 ± 0.06	1.37 ± 0.04	1.37 ± 0.07	1.65 ± 0.07	1.04 ± 0.04	0.80 ± 0.04	1.24 ± 0.09	40.0 ± 1.7
10-15	0.70	-	2.09 ± 0.07	1.43 ± 0.05	1.83 ± 0.07	2.08 ± 0.07	1.07 ± 0.02	0.80 ± 0.04	0.36 ± 0.04	11.9 ± 0.7
15-20	0.72	-	-	-	-	-	-	0.80 ± 0.04	-0.01 ± 0.035	-
20-25	0.71	-	-	-	-	-	-	0.80 ± 0.04	0.01 ± 0.03	-
25-29	0.71	-	-	-	-	-	-	0.80 ± 0.04	0.00 ± 0.03	n.d.

A dash indicates that no analysis has been made. n.d. = not detected.

* SBC = Soutar box core; HBC = Hessler box core.

** The values for ^{226}Ra reported here are averages determined in another core taken at the same time.

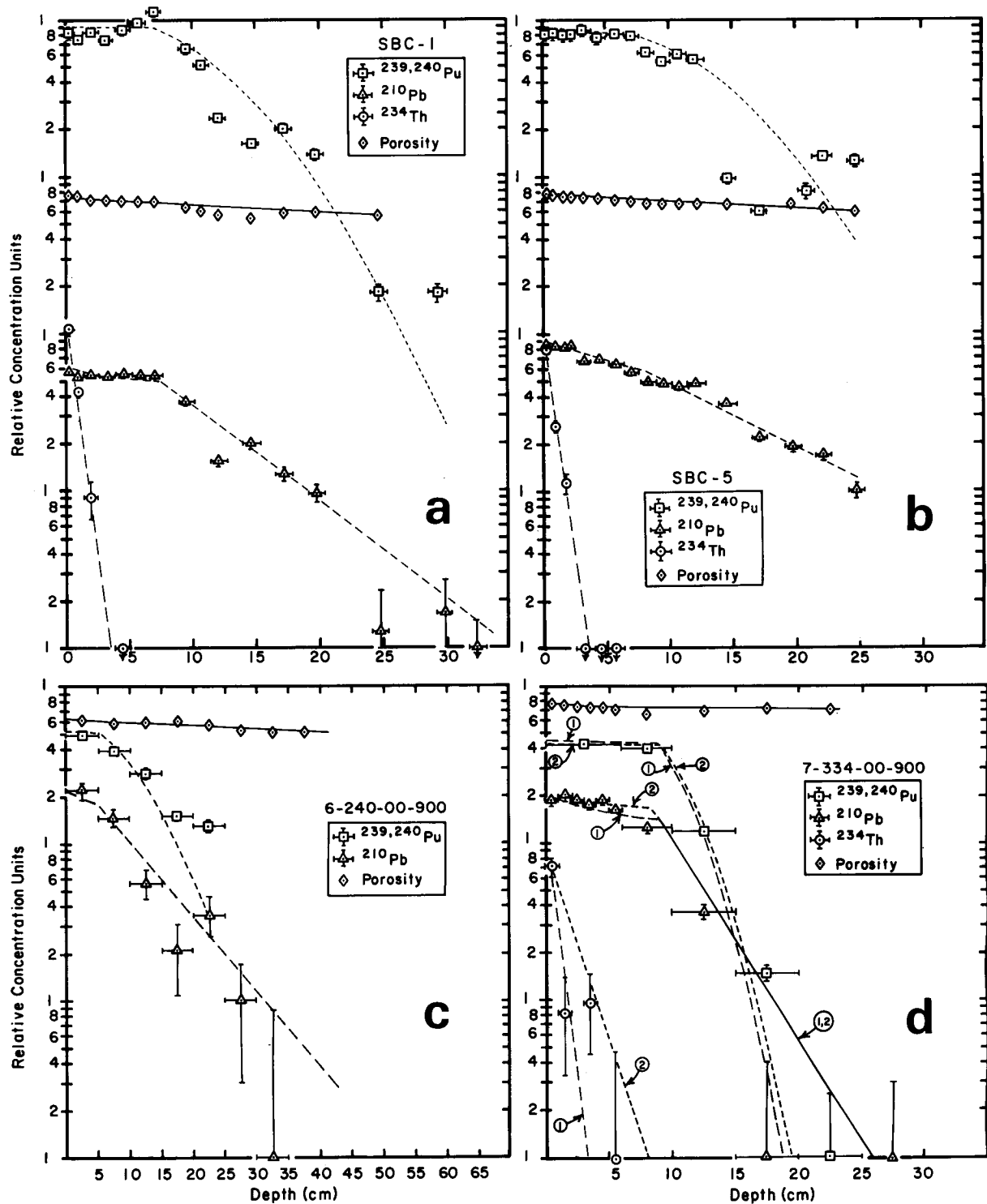


Fig. 6. For legend, see p. 259.

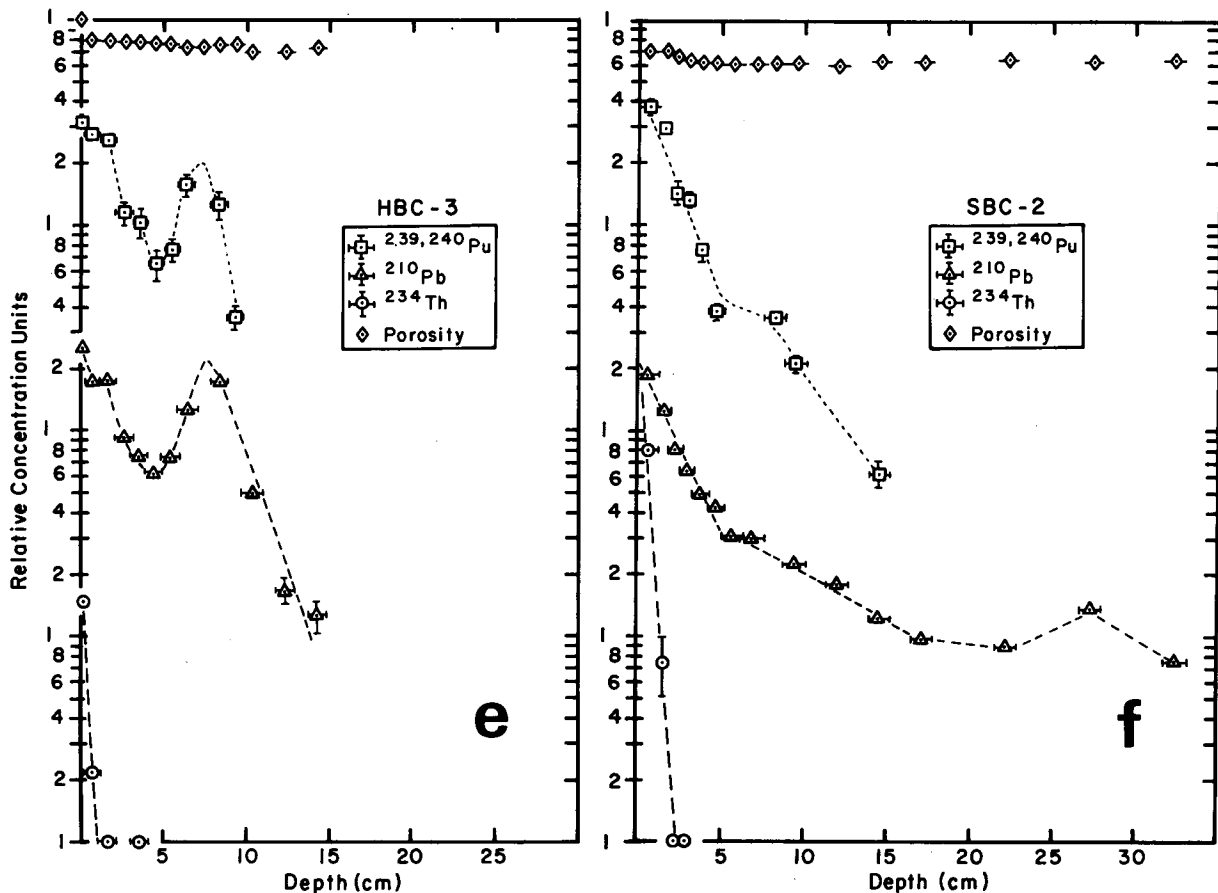


Fig. 6. Sediment analyses for $^{234}\text{Th}_{\text{xs}}$, $^{210}\text{Pb}_{\text{xs}}$, $^{239,240}\text{Pu}$ (all in dpm/g) and porosity (cm^3 water/ cm^3 wet sediment). Absolute values can be obtained from Table 3. Best fits from the numerical mixing and sedimentation model are shown for comparison (except for (e) and (f), where the lines connect only the data points). For 7-334-00-900, the two different mixing parameters in the top mixed layer, which have been used in the model runs (1) and (2), are given in Table 4.

out $^{239,240}\text{Pu}$ has already been removed to shelf sediments on very short time scales [24,31,32]. Our observations are consistent with evidence from other parts of the ocean [2,26,28], that an important fraction of $^{239,240}\text{Pu}$ in coastal waters is presently much less "particle-reactive" than when it was first introduced into the environment.

3.2. $^{239,240}\text{Pu}$ in sediments

The analytical results of plutonium isotopes and pertinent natural radioisotopes for four cores from the New York Bight south of Rhode Island and two cores from Narragansett Bay are summarized in Table 3. Locations of these cores are shown in Fig. 5. The

concentration profiles of $^{239,240}\text{Pu}$, excess ^{210}Pb and excess ^{234}Th in the various cores are also plotted in Fig. 6. As suggested by Benninger et al. [33], the cores from nearshore environments (SBC-1, -5, 6-240-00-900 and 7-334-00-900, see Fig. 6) can be separated into at least three layers. The top layer is a zone of rapid mixing where $^{210}\text{Pb}_{\text{xs}}$ and $^{239,240}\text{Pu}$ concentrations are more or less constant, and the $^{234}\text{Th}_{\text{xs}}$ decreases exponentially. The sediment mixing coefficient, or bioturbation rate (D_1) in this layer can be easily calculated by fitting the $^{234}\text{Th}_{\text{xs}}$ profile to the equation:

$$C_z = C_0 \exp \left[-z \left(\frac{\lambda}{D_1} \right)^{1/2} \right] \quad (1)$$

where λ = decay constant of ^{234}Th [34], z = depth (cm) and C_z and C_0 = concentrations at depth z and at the surface, respectively. The second layer is a zone of slower mixing where the $^{210}\text{Pb}_{\text{xs}}$ and $^{239,240}\text{Pu}$ concentrations decrease almost exponentially with depth. From the $^{210}\text{Pb}_{\text{xs}}$ profile in this layer, the apparent sedimentation rate (S_{app}) can be estimated by fitting the $^{210}\text{Pb}_{\text{xs}}$ profile to equation (2):

$$C_z = C_0 \exp(-\lambda z/S_{\text{app}}) \quad (2)$$

where λ = decay constant of ^{210}Pb [35]. The apparent sedimentation rate obtained this way is a maximum, since some of the $^{210}\text{Pb}_{\text{xs}}$ is mixed downward by the burrowing behavior of benthic macrofauna. The net sedimentation rate (S) and the sediment mixing coefficient in the second layer (D_{II}) can be estimated through simultaneous model fitting of $^{210}\text{Pb}_{\text{xs}}$ and $^{239,240}\text{Pu}$ profiles, as will be shown below. The third layer is a no-mixing zone where $^{210}\text{Pb}_{\text{xs}}$ and ^{14}C concentrations would, if available, decrease exponentially with depth due to sedimentation and radioactive decay only [35].

Fig. 7A summarizes our multi-box sediment mixing model which is similar to that of Peng et al. [36]. The time dependence of the concentration in the top box at a time step J is:

$$C_1^{J+1} = C_1^J + \frac{R_{\text{I}} \cdot \Delta t}{(1 - \phi_1) \cdot \rho \cdot \Delta z} [C_2 - C_1] - \frac{S \cdot \Delta t}{(1 - \phi_1) \cdot \rho \cdot \Delta z} [C_1 - C_0] - \lambda \cdot C_1 \cdot \Delta t \quad (3)$$

in the bottom box of the first layer:

$$(n = L_{\text{I}}/\Delta z)$$

$$C_n^{J+1} = C_n^J + \frac{R_{\text{I}} \cdot \Delta t}{(1 - \phi_n) \cdot \rho \cdot \Delta z} (C_{n-1} - C_n) + \frac{R_{\text{II}} \cdot \Delta t}{(1 - \phi_n) \cdot \rho \cdot \Delta z} (C_{n+1} - C_n) - \frac{S \cdot \Delta t}{(1 - \phi_n) \cdot \rho \cdot \Delta z} (C_n - C_{n-1}) - \lambda \cdot C_n \cdot \Delta t \quad (4)$$

in the bottom box of the second layer:

$$(m = (L_{\text{I}} + L_{\text{II}})/\Delta z)$$

$$C_m^{J+1} = C_m^J + \frac{R_{\text{II}} \cdot \Delta t}{(1 - \phi_m) \cdot \rho \cdot \Delta z} (C_{m-1} - C_m)$$

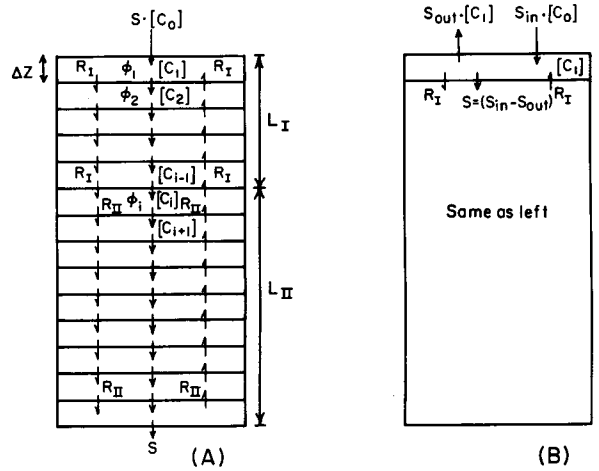


Fig. 7. The numerical mixing and sedimentation model is explained in A, and the model which includes resuspension of surface sediments in B.

$$- \frac{S \cdot \Delta t}{(1 - \phi_m) \cdot \rho \cdot \Delta z} (C_{m-1} - C_m) - \lambda \cdot C_m \cdot \Delta t \quad (5)$$

and in the rest of the boxes:

($i = 2$ to $n - 1$, or $n + 1$ to $m - 1$, respectively)

$$C_i^{J+1} = C_i^J + \frac{R_{\text{I}}(\text{or } R_{\text{II}}) \cdot \Delta t}{(1 - \phi_i) \cdot \rho \cdot \Delta z} (C_{i+1} + C_{i-1} - 2C_i) - \frac{S \cdot \Delta t}{(1 - \phi_i) \cdot \rho \cdot \Delta z} (C_{i-1} - C_i) - \lambda \cdot C_i \cdot \Delta t \quad (6)$$

where

- C = specific concentration in sediments (dpm/g dry sediment)
- C_0 = specific concentration on suspended particles (dpm/g dry sediment), assumed to be proportional to the input function
- S = constant sedimentation rate (g dry sediment/cm² yr)
- $R_{\text{I}}, R_{\text{II}}$ = constant sediment mixing rate in the first and second layers (g dry sediment/cm² yr)
- ϕ = porosity of sediment (cm³ water/cm³ wet sediment)
- ρ = density of dry sediments (2.5 g/cm³)
- Δz = depth step interval (0.3 cm)
- Δt = time step interval (1 day)
- $L_{\text{I}}, L_{\text{II}}$ = thickness of the first and second layer (cm).

The distinctive features of our model are:

(1) C , S and R are all expressed on a unit mass basis instead of the usual unit volume basis.

(2) The porosity profile is assumed to be in a steady state and can be expressed by $\phi = \phi_1 \exp(-\alpha \cdot z)$, where ϕ_1 = porosity at the core top, α = inverse of characteristic length, and z = depth.

(3) R can be related to the common diffusion coefficient, D , (cm^2/yr) by the relationship:

$$D = \frac{R \cdot \Delta z}{(1 - \phi) \rho} \quad (7)$$

Consequently, since the porosity decreases with depth, D also decreases with depth. The initial condition of our model is to set $C_i = 0$ at time zero. The

time dependence of C_0 (the specific concentration in the depositing sediment particles) is set constant for the simulation of the $^{210}\text{Pb}_{\text{xs}}$ profile. Our numerical model has been run for 200 years to attain steady state conditions as a check against the analytical solution for $^{210}\text{Pb}_{\text{xs}}$ profiles assuming constant porosity [33]. Differences were insignificant between the two models when the same parameters were used. For $^{239,240}\text{Pu}$ profiles, two boundary input functions were tried: (1) C_0 proportional to ^{90}Sr fallout in New York City [37] assuming a constant $^{239,240}\text{Pu}/^{90}\text{Sr}$ ratio (0.02), and (2) C_0 proportional to $^{239,240}\text{Pu}$ fallout as determined in a Greenland ice core [38]. Since the two input functions are similar, we found

TABLE 4

Parameters resulting from model runs which best fitted the radioisotope data of sediment cores *

Core no.	Water depth (m)	ϕ_1	α (cm^{-1})	L_I (cm)	L_{II} (cm)	$\Sigma^{234}\text{Th}_{\text{xs}}$ (dpm/ cm^2)	$\Sigma^{210}\text{Pb}_{\text{xs}}$ (dpm/ cm^2)	$\Sigma^{239,240}\text{Pu}$ (dpm/ cm^2)
<i>Narragansett Bay</i>								
6-240-00-900	10	0.63	0.0048	5	30	—	21	0.60
7-334-00-900	10	0.75	0.0020	9	30	3.9	15	0.42
<i>New York Bight</i>								
SBC-1	69	0.74	0.0105	7.5	30	6.7	58	0.93
SBC-5	87	0.80	0.0107	7.5	40	3.9	76	0.87
SBC-2	850	—	—	—	—	7.9	75	0.09
HBC-3	1800	—	—	—	—	0.3	80	0.05
	R_I (g/ cm^2 yr)	R_{II} (g/ cm^2 yr)	S (g/ cm^2 yr)	D_I^{**} (cm^2/yr)	D_{II}^{**} (cm^2/yr)	S' (cm/yr)	S_{app} (cm/yr)	
<i>Narragansett Bay</i>								
6-240-00-900	20.8 ± 5	7.2 ± 2	0.009 ± 0.03	7.5 ± 2.5	2.5 ± 0.6	0.01 ± 0.03	0.28 ± 0.07	
7-334-00-900								
(1)	9.4	0.64 ± 0.2	0.006 ± 0.03	5.0	0.32 ± 0.1	0.01 ± 0.03	0.10 ± 0.03	
(2)	59.1			31.5				
<i>New York Bight</i>								
SBC-1	20.9 ± 4	4.8 ± 1	0.009 (0–0.05)	10.7 ± 2	2.0 ± 0.4	0.01 (0–0.05)	0.23 ± 0.05	
SBC-5	5.7 ± 1	3.5 ± 0.9	0.140 ± 0.04	3.8 ± 0.8	1.7 ± 0.5	0.14 ± 0.04	0.32 ± 0.10	
SBC-2				1.3 ± 0.25			0.07 ± 0.015	
HBC-3				0.1 ± 0.05			0.05 ± 0.025	

* The meaning of the symbols is explained in the text. Indicated errors are estimated confidence levels based on simultaneously varying as many parameters as possible (uncertainty in input function not included) to best fit all radiotracer profiles equally well.

** D_I and S' are values at water-sediment interface, and D_{II} at the boundary between the top mixed layer and the second mixed layer (L_I).

no substantial differences between the $^{239,240}\text{Pu}$ model profiles using either input function. We therefore used New York City fallout values. This choice, we feel, is a realistic one because Noshkin and Bowen [24] and Livingston and Bowen [32] observed that Buzzards Bay sediments contained 80–90% of the total atmospheric fallout inventory for $^{239,240}\text{Pu}$ in 1964, just one year after the peak fallout of $^{239,240}\text{Pu}$. Input function (1) and (2) would both predict $80 \pm 10\%$ of the total fallout deposition for the year 1964. A comparison of the $^{239,240}\text{Pu}$ inventory in the two cores from the Buzzards Bay sediments taken in 1964 with 7 cores taken between 1972 and 1974 (both data sets from Livingston and Bowen [32]) indicates that this sedimentary basin did not accumulate Pu significantly between 1964 and 1974 (increase of only $20 \pm 20\%$).

The dotted or solid lines in Fig. 6a–d represent the best fit model curves (the model curves are always normalized to the observed surface concentration). The various parameters used or calculated are summarized in Table 4. In shallow coastal environments (<100 m) the thickness of the surface rapid mixing layer, L_I , can vary from a few centimeters to 10 cm, and its mixing coefficient, R_I , from 6 to 60 $\text{g}/\text{cm}^2 \text{ yr}$ (or $D_I = 4\text{--}32 \text{ cm}^2/\text{yr}$ at the sediment-water interface). The thickness of the second layer, L_{II} , can be as great as 30 cm, and its mixing coefficient, R_{II} , varies from 0.6 to 7 $\text{g}/\text{cm}^2 \text{ yr}$ (or $D_{II} = 0.3\text{--}2.5 \text{ cm}^2/\text{yr}$ at the depth L_I). L_{II} has been chosen to extend to a depth where both $^{239,240}\text{Pu}$ and $^{210}\text{Pb}_{\text{xs}}$ activities become non-detectable (by actual measurement or by extrapolation). Our model is not sensitive to L_{II} . However, the selection of L_I is of critical importance for both profiles, and is one of the parameters resulting from the simultaneous model fitting of the $^{210}\text{Pb}_{\text{xs}}$ and $^{239,240}\text{Pu}$ profiles.

Our estimates of recent sedimentation rates for the “mud hole” area of the New York Bight, south of Rhode Island, agree well with those of Bothner et al. [39], which were derived using ^{14}C (0.025 cm/yr). The most interesting result is that the sedimentation rates obtained from our model (see S and S' in Table 4) are always much lower than the apparent sedimentation rate, S_{app} , obtained from $^{210}\text{Pb}_{\text{xs}}$ profiles alone, even though the uncertainties in S and S' are large (Table 4). Very similar results were obtained by Benninger et al. [33] from a Long Island Sound

core. They gave $D_I = 6\text{--}38 \text{ cm}^2/\text{yr}$, $D_{II} = 0.6\text{--}1.0 \text{ cm}^2/\text{yr}$ and $S' < 0.05 \text{ cm}/\text{yr}$ compared to $S_{\text{app}} = 0.11 \text{ cm}/\text{yr}$, assuming porosity to be constant with depth. Therefore, as cautioned by Benninger et al. [33], one should be very careful about using S_{app} to estimate the actual net accumulation rate of sediments and the pollutants they contain in coastal marine environments, where the effect of sediment mixing has often been neglected in the past (e.g. [40]). In order to obtain reliable S or S' , we would need a longer core (down to the historic layer where bioturbational mixing is absent) and use the ^{14}C dating technique.

The somewhat irregular shape (subsurface maxima) of the $^{239,240}\text{Pu}$ profiles in Fig. 6 is probably caused by the variable feeding and burrowing behavior of benthic macrofauna [33,34].

The cumulative $^{239,240}\text{Pu}$ deposition is about $0.44 \pm 0.11 \text{ dpm}/\text{cm}^2$ in the northern latitude between 30° and 50°N [1]. Narragansett Bay, then, has accumulated approximately 100% of atmospheric fallout $^{239,240}\text{Pu}$, and the New York Bight shelf sediments contain almost twice the atmospheric fallout inputs (Table 4). With very low net sediment accumulation rates (<0.03 $\text{g}/\text{cm}^2 \text{ yr}$), how can the coastal sediments efficiently accumulate $^{239,240}\text{Pu}$? The following is our explanation: Let us consider a thin layer of well-mixed sediments at the water-sediment interface (Fig. 7B). The sediments continuously receive settling particles from the water column at a sedimentation rate of S_{in} ($\text{g}/\text{cm}^2 \text{ day}$) and a specific $^{239,240}\text{Pu}$ activity of C_0 (dpm/g). Sediment particles are resuspended into the water column at a resuspension rate of S_{out} and specific $^{239,240}\text{Pu}$ activity equal to that in the top sediments (C_1). The net gain of $^{239,240}\text{Pu}$ by sediments F_{net} , is:

$$F_{\text{net}} = S_{\text{in}} \cdot C_0 - S_{\text{out}} \cdot C_1 \\ = S \cdot C_0 + S_{\text{out}}(C_0 - C_1) \quad (8)$$

where $S = S_{\text{in}} - S_{\text{out}}$ (net sedimentation rate). Remobilization of soluble Pu is neglected in this model, since it is probably insignificant compared to the total sediment inventory as shown above. Two terms contribute to the accumulation of Pu in the sediments. The first term is simply the burial of Pu adsorbed on particles through net sedimentation ($S \cdot C_0$). The second term reflects the fact that a fraction of the particles which are resuspended to the

overlying water column is mixed down into the sediments by bioturbation and therefore creates a concentration gradient ($C_0 - C_1$) between freshly sedimented and resuspended particles. Therefore, the flux of Pu also increases with the sediment resuspension rate S_{out} and with the concentration gradient $C_0 - C_1$, both of which are affected by the bioturbation rate of bottom sediments: an increase in the benthic fauna activities increases both the sediment mixing rate (R) and the sediment mixing depth, which tend to decrease C_1 (due to mixing with less contaminated sediments below), thus making the ($C_0 - C_1$) term larger. The churning of the surface sediments by benthic fauna can increase the erodibility of the surface sediments and, therefore, the resuspension rate

of sediments [41]. The resuspended sediment particles, in turn, scavenge more "particle-reactive" pollutants from the water column down to the water-sediment interface. Though there are not many measurements of S_{out} and R to quantify the benthic faunal activity in sediments, the penetration depth of $^{239,240}\text{Pu}$ in sediments, L_p , (defined here as the depth at which the concentration of $^{239,240}\text{Pu}$ is about 5% of that in surface sediment) can be roughly taken as an indicator for the intensity of benthic faunal activity. The linear correlation between the total cumulative inventory of $^{239,240}\text{Pu}$ ($\Sigma^{239,240}\text{Pu}$ dpm/cm²) and L_p (but not with the net sedimentation rate) for nearshore and offshore cores (Fig. 8) supports our contention that the accumulation of plutonium in marine sediments is modulated by benthic faunal activity.

The surface shelf sediments from the New York Bight south of Rhode Island are high in fine-grained particles (greater than 20% by weight in particle size $<63 \mu\text{m}$). Therefore, the area was nicknamed the "mud hole" [42]. But the total area of the "mud hole" is not more than 20% of the whole New York Bight Shelf area [43]. The rest of the shelf is mainly sandy (less than 10% by weight in particle size $<63 \mu\text{m}$). Since the "mud hole" sediments have accumulated at most only about twice the atmospheric fall-out input of $^{239,240}\text{Pu}$, one would expect the sandy sediments to accumulate some of the atmospheric $^{239,240}\text{Pu}$ inputs. Unfortunately, we have no sediment core samples from those areas. Also, most of the atmospheric $^{239,240}\text{Pu}$ inputs to the shelf may have been deposited in the bays along the shore or transported out to the slope areas by currents. Further studies are needed.

A few final comments on our two cores from the New York Bight slope area (Fig. 6e, f) are necessary: The mid-depth maxima of $^{210}\text{Pb}_{xs}$ and $^{239,240}\text{Pu}$ in core HBC-3 from the continental slope suggest a very recent slumping of sediments, probably caused by turbidites. Subsequent bioturbation of variable intensity would smooth out the original signal in such a way as to suggest an increase in apparent sedimentation rates with depth. The occurrence of $^{239,240}\text{Pu}$ at depth in these two cores indicates that these slumping events must have occurred within the last 15 years. Alternative explanations such as bioturbation alone or analytical and sampling errors cannot be excluded.

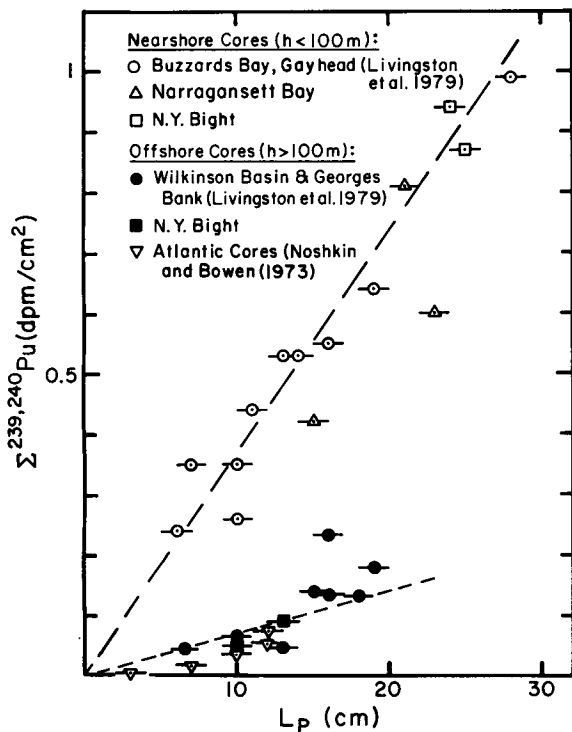


Fig. 8. $^{239,240}\text{Pu}$ inventories in coastal marine sediments versus the depth (L_p) where $^{239,240}\text{Pu}$ activities are below 5% of the surface activities. For Narragansett Bay, one core described by Goldberg [40] and re-evaluated by Santschi [44] has been included.

4. Conclusions

The apparent correlation between "dissolved" $^{239,240}\text{Pu}$ ($<0.45\ \mu\text{m}$) and the suspended particle concentrations in the New York Bight nearshore and Narragansett Bay waters can be best explained by the injection of more soluble, less reactive species (anionic Pu (V + VI) or colloidal (Pu (III + IV) species) from the bottom sediments to the overlying water column during the resuspension of surface sediments in warmer seasons. $^{239,240}\text{Pu}$ input and output fluxes in the New York Bight waters can be approximately balanced if it is assumed that (1) only about 15–20% of the total $^{239,240}\text{Pu}$ is "particle-reactive" as Pu (III + IV), and (2) Pu (III + IV) behaves similarly to Th (IV) and is therefore removed at a similar rate from the surface waters to the sediments.

Our estimates of recent sedimentation rates for the "mud hole" areas in the New York Bight, south of Rhode Island, agree well with those of Bothner et al. [39], which were derived using ^{14}C dating techniques (0.025 cm/yr). Despite the very low net sediment accumulation rates of approximately zero to less than 0.03 cm/yr which were often found in the New York Bight shelf area south of Rhode Island and Narragansett Bay, and of less than 0.05 cm/yr in Long Island Sound [33], the cumulative $^{239,240}\text{Pu}$ inventories in these areas are between one and two times the atmospheric fallout inputs. The continuous resuspension of particles from surface sediments, which adsorb $^{239,240}\text{Pu}$ from the water column, and sediment mixing by bioturbation, which effectively mixes and dilutes the polluted surface sediments with less contaminated sediments below, can explain the observed high sedimentary inventory and deep penetration of $^{239,240}\text{Pu}$ in these areas

Acknowledgements

We wish to thank Dr. Pierre Biscaye, George Hampson and Steve Carson for their assistance in sediment core sampling. We have benefitted from useful criticisms by Mike Amdurer, Dennis Adler and three unknown reviewers. In addition, the cooperation of the crew members of R/V "Conrad" and R/V "Cape Henlopen" is greatly appreciated.

This research is supported by a grant from the Department of Energy (EY-76-S-02-2185).

References

- 1 E.P. Hardy, P.W. Krey and H.L. Volchok, Global inventory and distribution of fallout plutonium, *Nature* 241 (1973) 444–445.
- 2 J.A. Hetherington, The behavior of plutonium nuclides in the Irish Sea, in: *Environmental Toxicity of Aquatic Radionuclides*, M.W. Miller and J.N. Stanard, eds. (Ann Arbor Science Publishers, Ann Arbor, Mich., 1975) 81–106.
- 3 P.H. Santschi, Y.H. Li and J. Bell, Natural radionuclides in the water of Narragansett Bay, *Earth Planet. Sci. Lett.* 45 (1979) 201–213.
- 4 A. Kaufman, Y.H. Li and K.K. Turekian, The removal rates of ^{234}Th and ^{228}Th from waters of the New York Bight (submitted to *Earth Planet. Sci. Lett.*).
- 5 Y.H. Li, P.H. Santschi, A. Kaufman, L.K. Benninger and H.W. Feely, ^{228}Th - ^{228}Ra radioactive disequilibrium in the New York Bight during winter and spring seasons (submitted to *Earth Planet. Sci. Lett.*).
- 6 K.M. Wong, Radiochemical determination of Pu in seawater, sediments and marine organisms, *Anal. Chim. Acta* 56 (1971) 355–364.
- 7 H.J. Simpson, R.M. Trier and C.R. Olsen, in: *Transuranic Elements in the Environment*, W.S. Hanson, ed., U.S. Dep. Energy Publ. TID-22800 (1980) 684–690.
- 8 W.S. Broecker, A. Kaufman and R.M. Trier, The residence times of thorium in surface seawater and its implications regarding the fate of reactive pollutants, *Earth Planet. Sci. Lett.* 20 (1973) 35–44.
- 9 R. Aller and T.K. Cochran, ^{234}U / ^{238}U disequilibrium in nearshore sediments: particle reworking and diagenetic time scales, *Earth Planet. Sci. Lett.* 29 (1976) 37–50.
- 10 T.L. Ku, Uranium series disequilibrium in deep sea sediments, Ph.D. Thesis, Columbia University (1966).
- 11 G.W. Kipphut, An investigation of sedimentary processes in lakes, Ph.D. Thesis, Columbia University (1978).
- 12 L.K. Benninger, The uranium-series radionuclides as tracers of geochemical processes in Long Island Sound, Ph.D. Thesis, Yale University (1976).
- 13 G.G. Mathieu, ^{222}Rn and ^{226}Ra technique of analysis, Prog. Rep., ERDA Contract EY 76-S-02-2185 (1977).
- 14 H.L. Volchok and M. Feiner, A radioanalytical laboratory intercomparison exercise, U.S. Dep. Energy, Environmental Measurements Laboratory, EML-366 (1979).
- 15 S.R. Aston, Evaluation of the chemical forms of Pu in seawater, *Mar. Chem.* 8 (1980) 319–326.
- 16 M.A. Wahlgren, K.A. Orlandini, D.M. Nelson and R.P. Larsen, Oxidation state characteristics of $^{239,240}\text{Pu}$ in selected North American freshwaters (submitted for publication).
- 17 E.A. Bondietti, J.R. Trabalka, Evidence for plutonium (V) in an alkaline freshwater pond, *Radiochem. Radioanal. Lett.* 42 (1980) 169–176.
- 18 D.M. Nelson and M.B. Lovett, Oxidation state of Pu in the Irish Sea, *Nature* 276 (1978) 599–601.
- 19 Y.H. Li, H.W. Feely and P.H. Santschi, ^{228}Th - ^{228}Ra

- radioactive disequilibrium in the New York Bight and its implication for coastal pollution, *Earth Planet. Sci. Lett.* 42 (1979) 13–26.
- 20 P.H. Santschi, D. Adler, M. Amdurer, Y.H. Li and J. Bell, Thorium isotopes as analogues for “particle-reactive” pollutants in coastal marine environments, *Earth Planet. Sci. Lett.* 47 (1980) 327–335.
 - 21 J.J. Higgs, R.D. Cherry, M. Heyraud and S.W. Fowler, Rapid removal of plutonium from the oceanic surface layer by zooplankton fecal pellets, *Nature* 266 (1971) 623–624.
 - 22 F.G. Lowman, T.R. Rice and F.A. Richards, Accumulation and redistribution of radionuclides by marine organisms, in: *Radioactivity in the Marine Environment* (National Academy of Sciences, Washington, D.C., 1971) 161–199.
 - 23 J.J. Walsh, T.E. Whittleage, F.W. Barvenik, C.D. Wirik, S.O. Howe, W.E. Esaias and J.T. Scott, Wind events and food chain dynamics within the New York Bight, *Limnol. Oceanogr.* 23 (1978) 659–683.
 - 24 V.E. Noshkin and V.T. Bowen, Concentrations and distributions of long-lived fallout radionuclides in open ocean sediments, *IAEA-SM-158/45* (1973) 671–686.
 - 25 L.D. Labeyrie, H.D. Livingston and V.T. Bowen, Comparison of the distributions in marine sediments of the fallout-derived nuclides ^{55}Fe and $^{239,240}\text{Pu}$: a new approach to the chemistry of environmental radionuclides, in: *Transuranium Nuclides in the Environment*, *IAEA-SM-199/115* (1976) 121–135.
 - 26 V.T. Bowen, V.E. Noshkin, H.D. Livingston and H.L. Volchok, Fallout radionuclides in the Pacific Ocean; vertical and horizontal distributions, largely from GEOSECS stations, *Earth Planet. Sci. Lett.* 49 (1980) 411–434.
 - 27 H.W. Feely, H.L. Volchok, E.P. Hardy and L.E. Toonkel, Worldwide deposition of ^{90}Sr trough 1976, *Environ. Sci. Technol.* 12 (1978) 808–809.
 - 28 C.D. Bue, Streamflow from the United States into the Atlantic Ocean during 1931–1960, *U.S. Geol. Surv., Water Supply Paper 1899-1* (1970) 36 pp.
 - 29 M.A. Wahlgren, J.R. Robbins and D.N. Edgington, in *Transuranic Elements in the Environment*, W.S. Hanson, ed., U.S. Dep. Energy Publ. TID-22800 (1980) 659–683.
 - 30 V.T. Bowen, K.M. Wong and V.E. Noshkin, Plutonium-239 in and over the Atlantic Ocean, *J. Mar. Res.* 29 (1971) 1–10.
 - 31 V.T. Bowen, H.D. Livingston and J.C. Burke, Distributions of transuranium nuclides in sediments and biota in the North Atlantic Ocean, in: *Transuranium Nuclides in the Environment*, *IAEA-SM-199/96* (1976) 107–118.
 - 32 H.D. Livingston and V.T. Bowen, Pu and ^{137}Cs in coastal sediments, *Earth Planet. Sci. Lett.* 43 (1979) 29–45.
 - 33 L.K. Benninger, R.C. Aller, J.K. Cochran and K.K. Turekian, Effects of biological sediment mixing on the ^{210}Pb chronology and trace metal distribution in a Long Island Sound sediment core, *Earth Planet. Sci. Lett.* 43 (1979) 241–259.
 - 34 R.C. Aller, The influence of macrobenthos on chemical diagenesis of marine sediments, Ph.D. Thesis, Yale University (1977).
 - 35 M. Koide, A. Soutar and E.D. Goldberg, Marine geochronology with Pb-210, *Earth Planet. Sci. Lett.* 14 (1972) 442–446.
 - 36 T.H. Peng, W.S. Broecker and W.H. Berger, Rates of benthic mixing in deep sea sediment as determined by radio-active tracers, *Quat. Res.* 11 (1979) 141–149.
 - 37 HASL, Final tabulation of monthly ^{90}Sr fallout data: 1954–1976. U.S. Energy Res. Dev. Adm., HASL-329 (1977) 401 pp.
 - 38 M. Koide, E.D. Goldberg, M.M. Herron and C.C. Langway, Jr., Transuranic depositional history in South Greenland layers, *Nature* 269 (1977) 137–139.
 - 39 M.H. Bothner, E.C. Spiker, P.P. Johnson, R.R. Rendigs and P.J. Aruscavage, Geochemical evidence for modern sediment accumulation on the continental shelf off southern New England, *J. Sediment. Petrol.* (in press).
 - 40 E.D. Goldberg, E. Gamble, J.J. Griffin and M. Koide, Pollution history of Narragansett Bay as recorded in its sediments, *Estuarine Coastal Mar. Sci.* 5 (1977) 549–561.
 - 41 D.C. Rhoads, J.Y. Yingst and W.J. Ullman, Seafloor stability in central Long Island Sound, 1. Temporal changes in erodibility of fine-grained sediments, in: *Estuarine Interactions*, M.L. Wiley, ed. (Academic Press, New York, N.Y., 1978) 221–244.
 - 42 P.E. Biscaye, C.R. Olsen and G. Mathieu, Suspended particulate matter and natural radionuclides as tracers of pollutant transports in continental shelf water of the eastern U.S., in: *First American-Soviet Symposium on Chemical Pollution of the Marine Environment*, EPA-600/9-78-038 (1978) 125–147.
 - 43 J. Schlee, Atlantic Continental Shelf and Slope of the United States – Sediment texture of the northeastern part, *U.S. Geol. Surv. Prof. Paper 529-L* (1973) 64 pp.
 - 44 P.H. Santschi, A revised estimate of trace metal fluxes to Narragansett Bay, *Estuarine Coastal Mar. Sci.* 11 (1980) 115–118.